Supplement of Atmos. Chem. Phys., 24, 3217–3240, 2024
https://doi.org/10.5194/acp-24-3217-2024-supplement

Atmospheric Chemistry and Physics
Open Access
EGU

Supplement of

Impacts of ice-nucleating particles on cirrus clouds and radiation derived from global model simulations with MADE3 in EMAC

Christof G. Beer et al.

Correspondence to: Christof G. Beer (christof.beer@dlr.de)

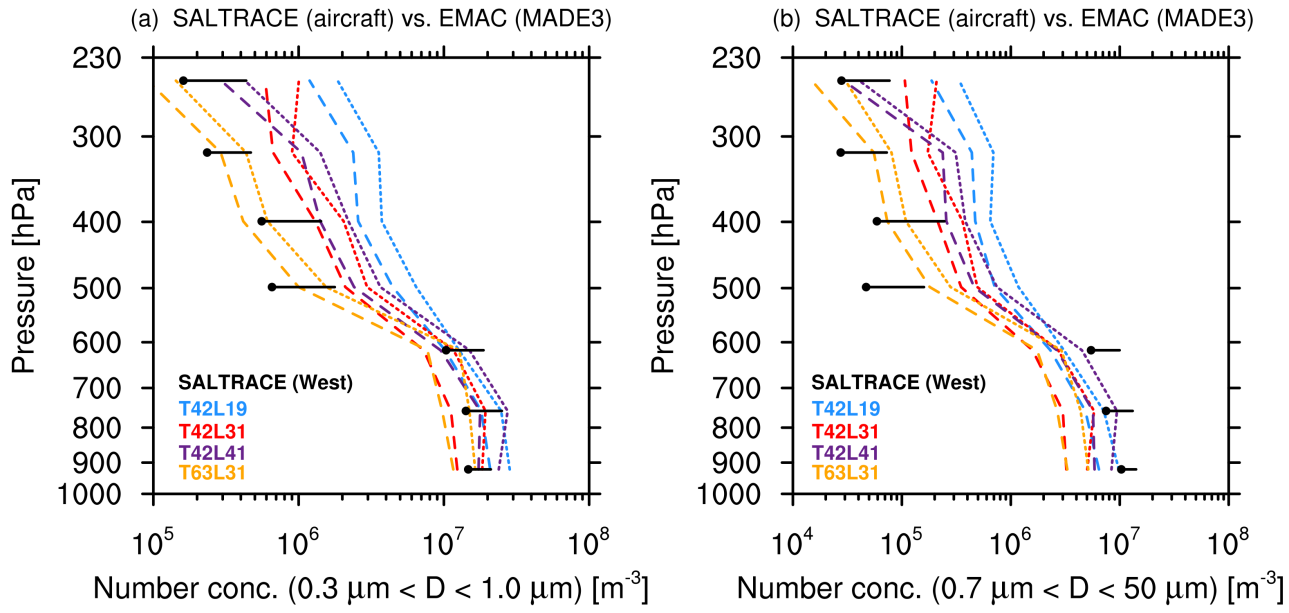

Figure S1. Similar to Fig. 5 of Beer et al. (2020), comparing different observational data from the SALTRACE mineral dust campaign (June–July 2013) with model results from simulations with different horizontal and vertical grid resolutions. Dots represent mean values; whiskers represent standard deviations of observations (only positive direction shown). Mean values (long-dashed lines) and standard deviations (short-dashed lines) of the model results are shown for the different model resolutions: T42L19 (blue), T42L31 (red), T42L41 (purple), and T63L31 (orange). (a) Total aerosol number concentration for particles with diameters in the range $0.3\ \mu\text{m} < D < 1\ \mu\text{m}$. (b) Similar to (a), but considering larger particles in the diameter range $0.7\ \mu\text{m} < D < 50\ \mu\text{m}$.

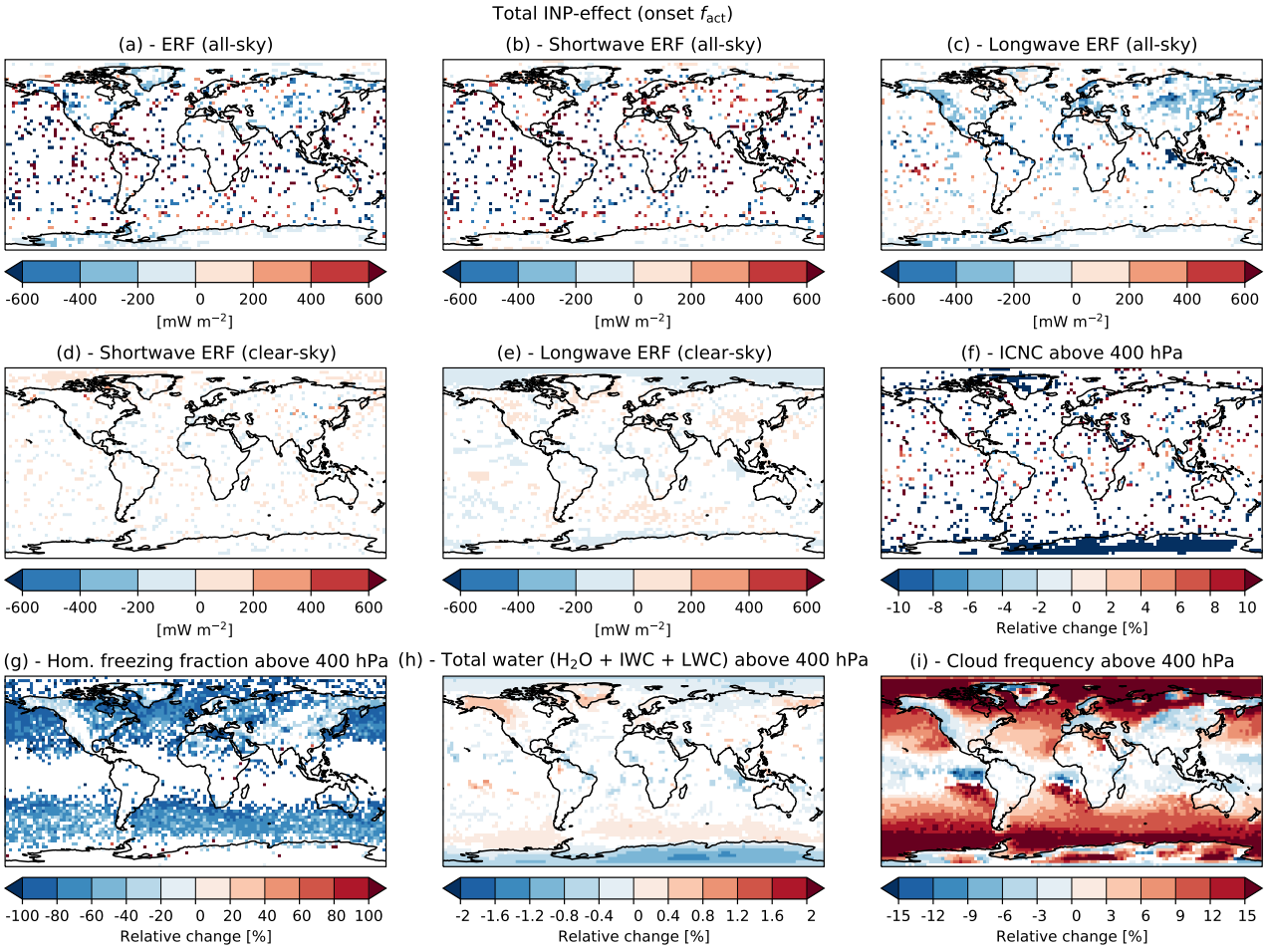

Figure S2. As in Fig. 1, but showing the geographic distribution of the simulated total INP-cirrus effect on the different radiation and cloud variables considering all INP types. Panels (a-e) represent radiative forcings at the top of the atmosphere, panels (f-i) show averaged cloud properties above 400 hPa.

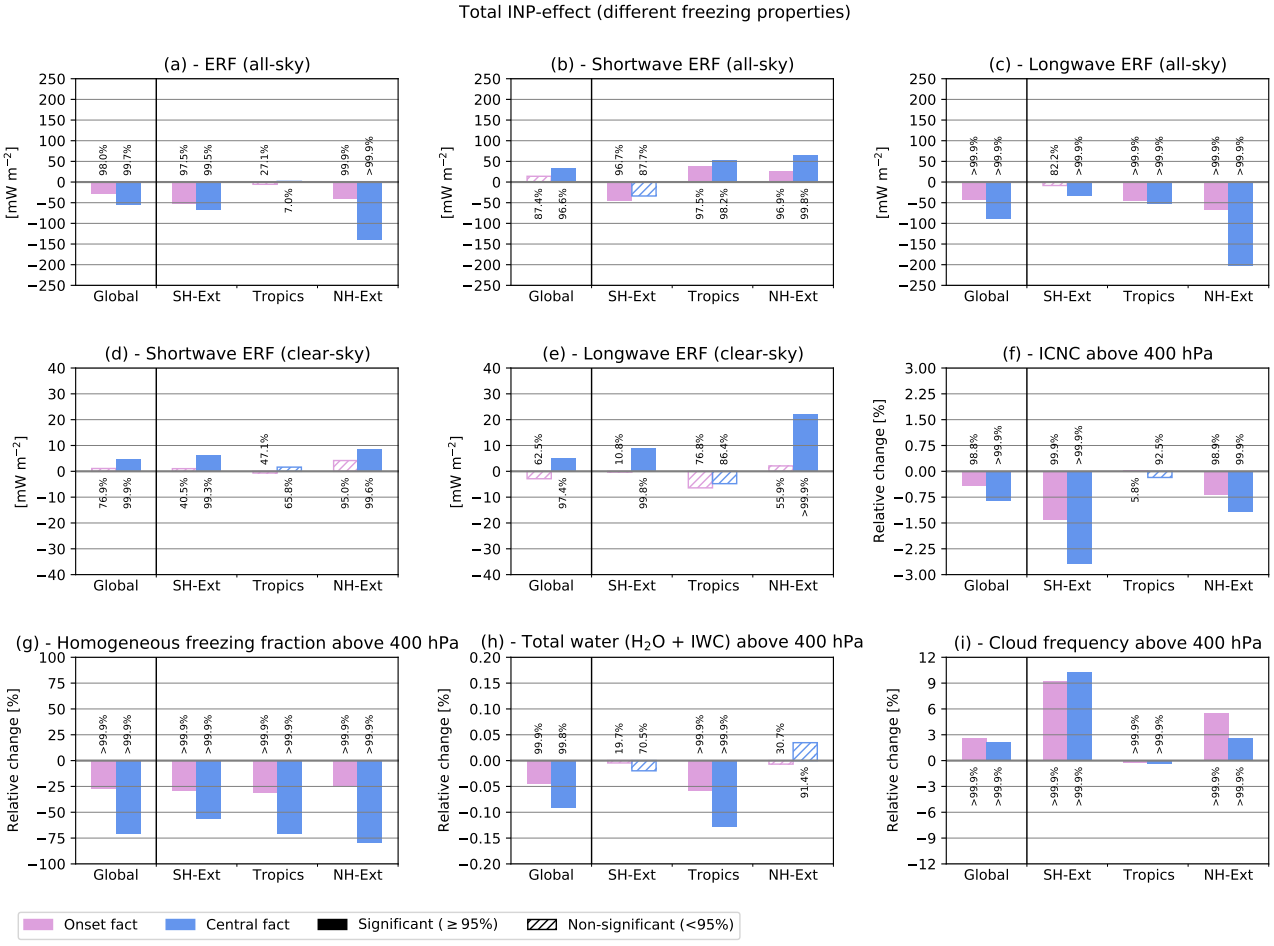

Figure S3. As in Fig. 2, but additionally showing all simulated variables from Fig. 1.

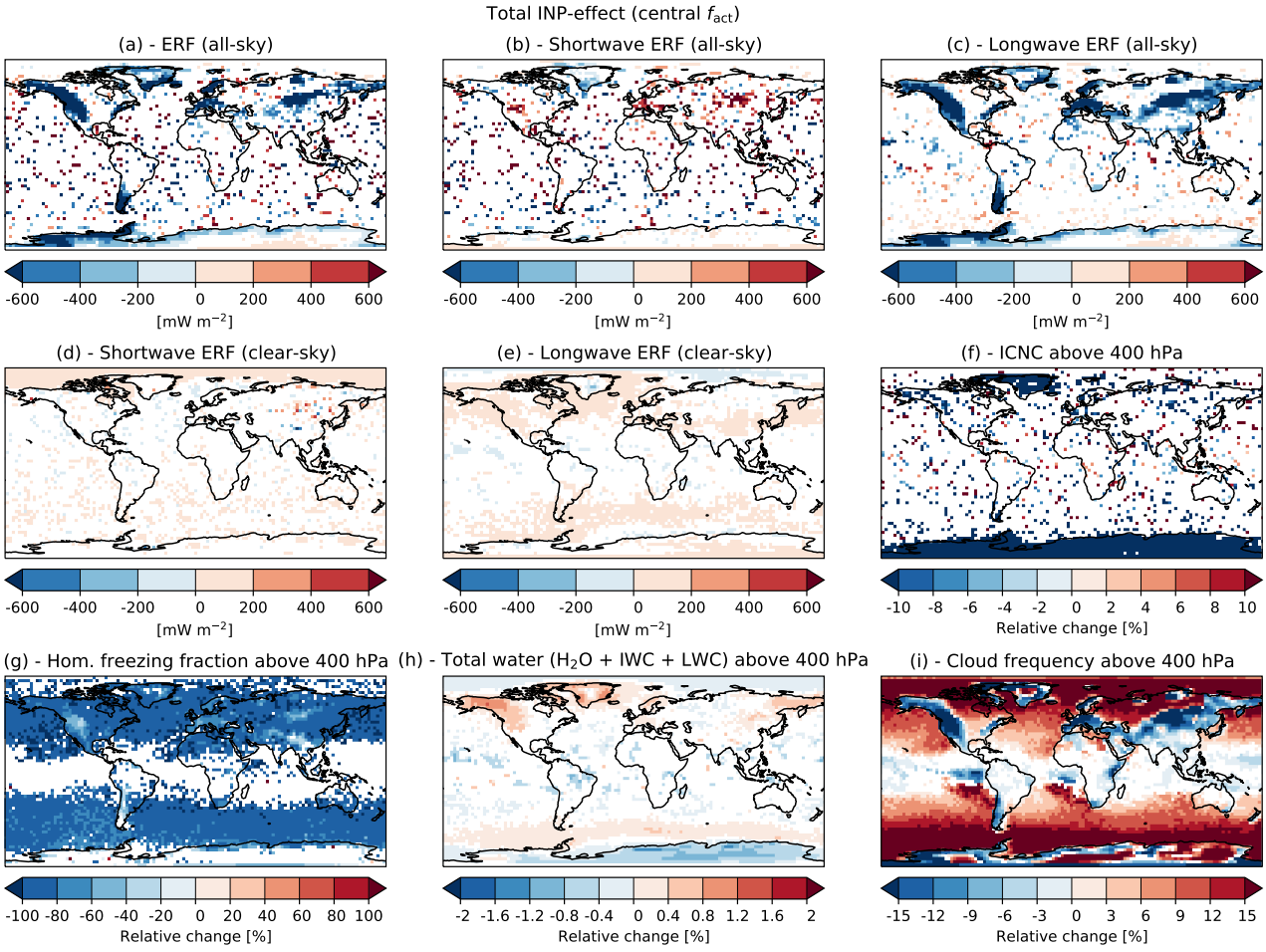

Figure S4. As in Fig. S3, but showing the geographic distribution of the simulated total INP-cirrus effect on the different radiation and cloud variables considering all INP types and an increased freezing potential of INPs (central f_{act}). Panels (a-e) represent effective radiative forcings at the top of the atmosphere, panels (f-i) show averaged cloud properties above $400\,\mathrm{hPa}$.

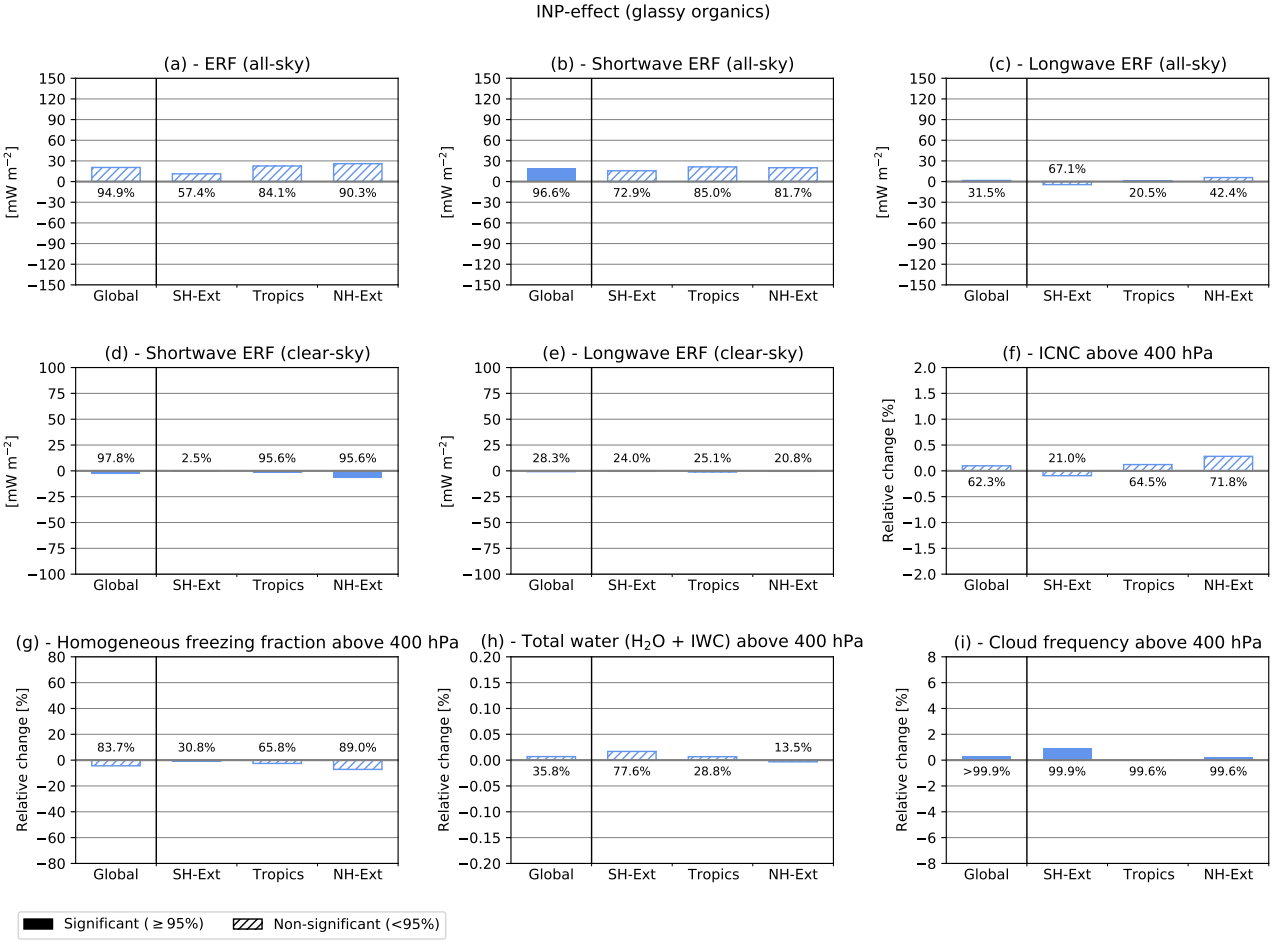

Figure S5. As in Fig. 4, but showing the INP-cirrus effect induced by glassy organics, calculated from the difference between a simulation including glPOM, DU and BC INPs, and a simulation including only heterogeneous freezing on DU and BC.

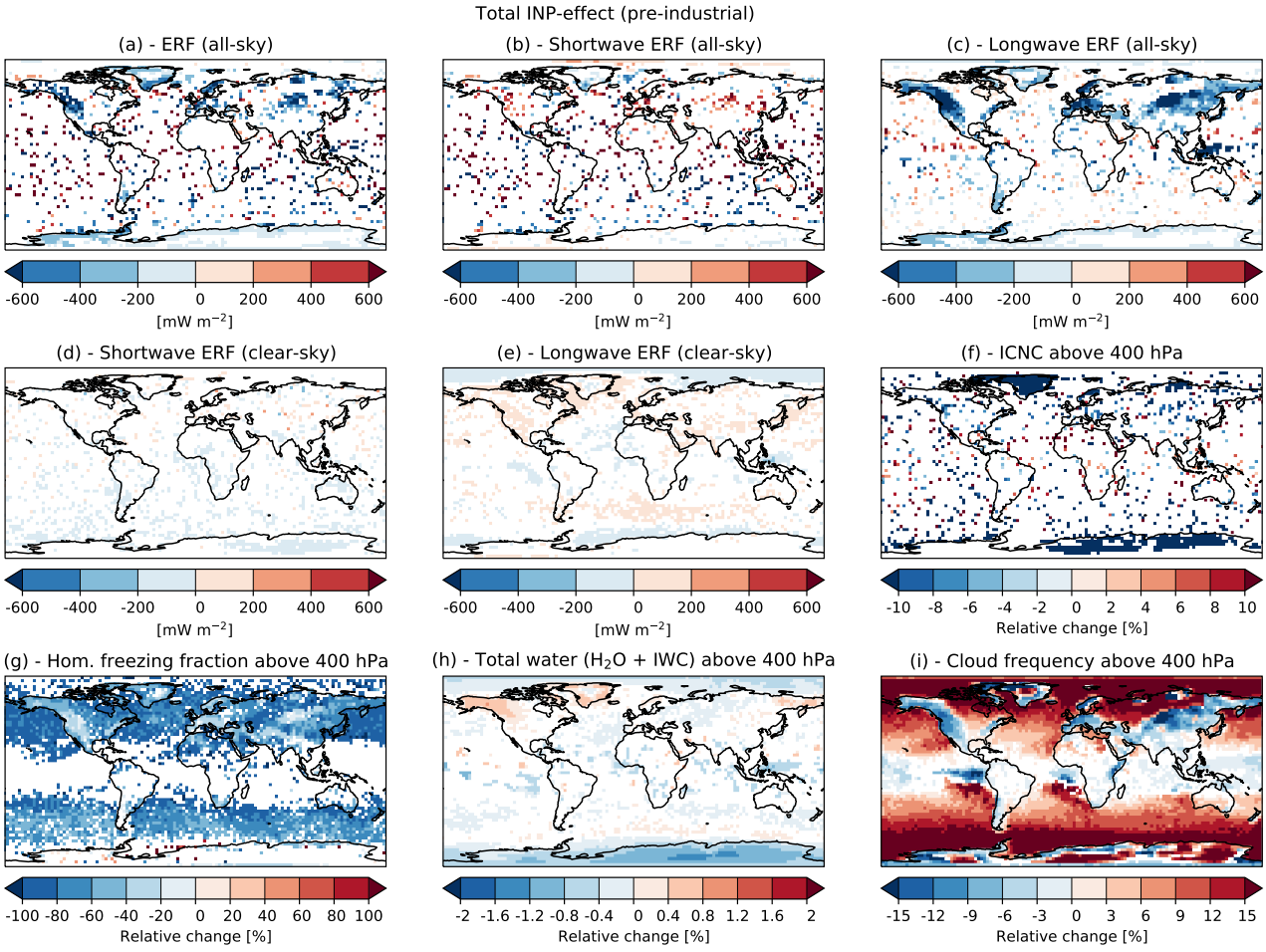

Figure S6. As in Fig. S4, but showing the geographic distribution of the simulated total INP-cirrus effect on the different radiation and cloud variables considering pre-industrial (1750) conditions. Panels (a-e) represent effective radiative forcings at the top of the atmosphere, panels (f-i) show averaged cloud properties above 400 hPa.

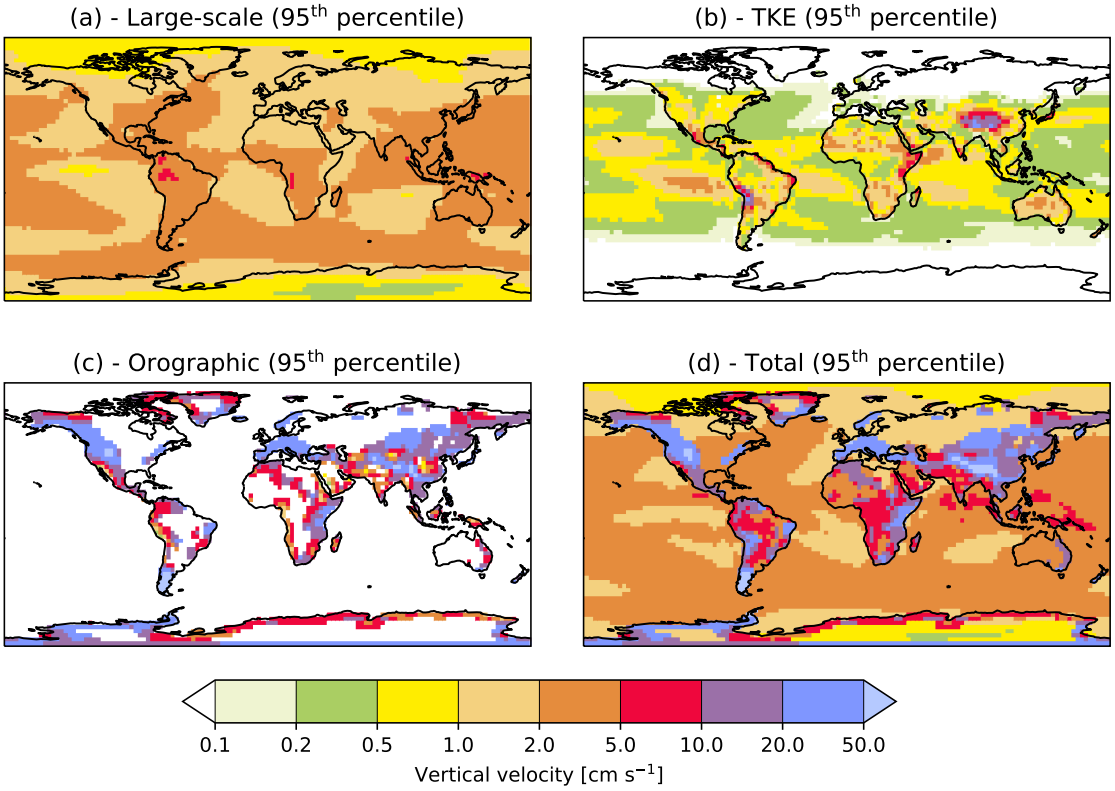

Figure S7. Similar to Fig. 2 of Righi et al. (2021), showing the vertical velocity components considered by the model: (a) large-scale, (b) subgrid-scale using the turbulent kinetic energy (TKE) as proxy, (c) subgrid-scale contribution of the orographic gravity waves in the vicinity of mountain ranges, and (d) the total vertical velocity as the sum of the three components. Each panel shows the 95th percentile of the vertical velocity distribution with respect to time (considering the 2001–2010 simulation period) and vertical (above 400 hPa) coordinates.

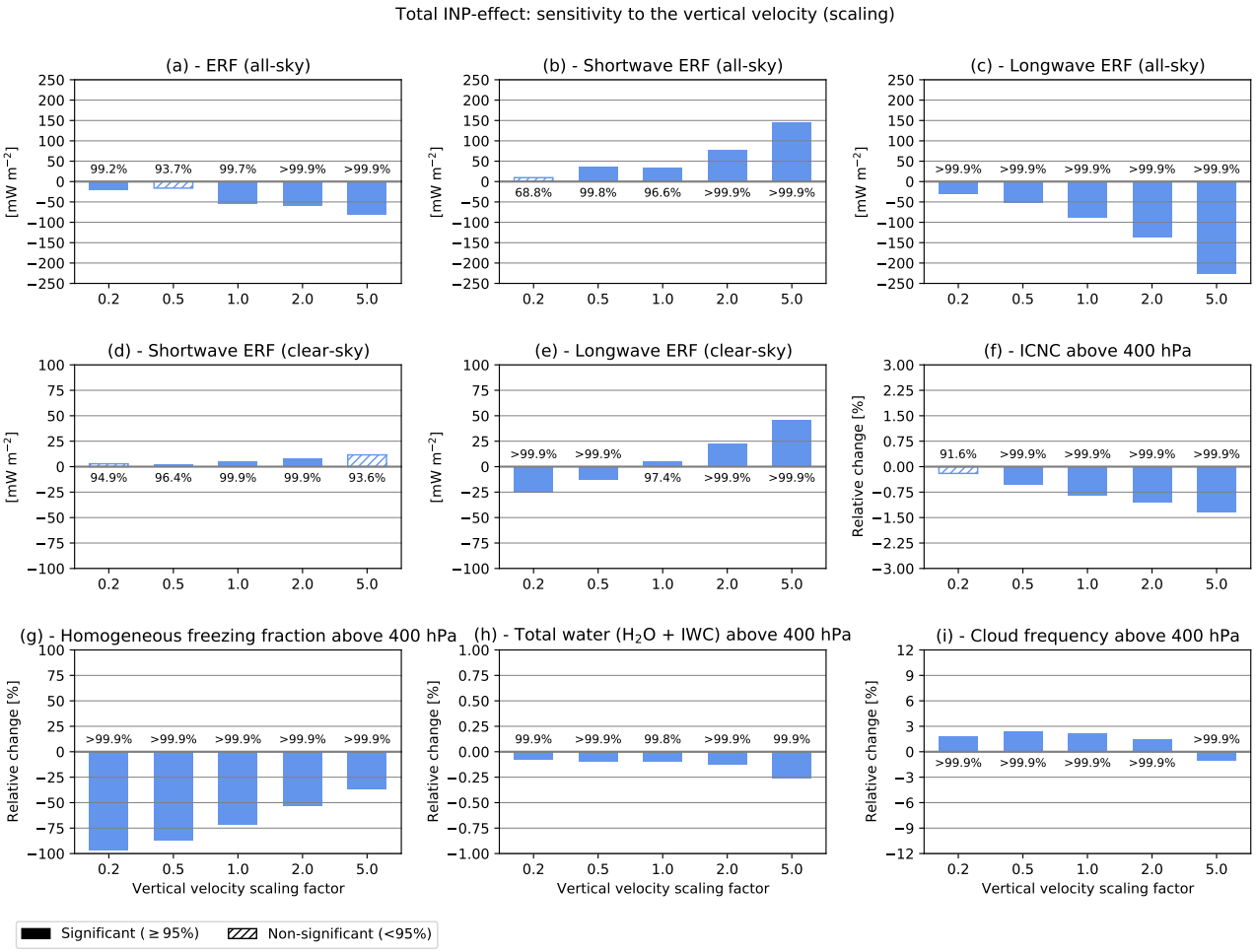

Figure S8. As in Fig. 6, but showing the sensitivity of the total INP-cirrus effect (enhanced ice-nucleating properties of INPs) to the scaling of the parametrized vertical velocity considering scaling factors of 0.2, 0.5, 1.0 (i.e. the reference case), 2.0, and 5.0.

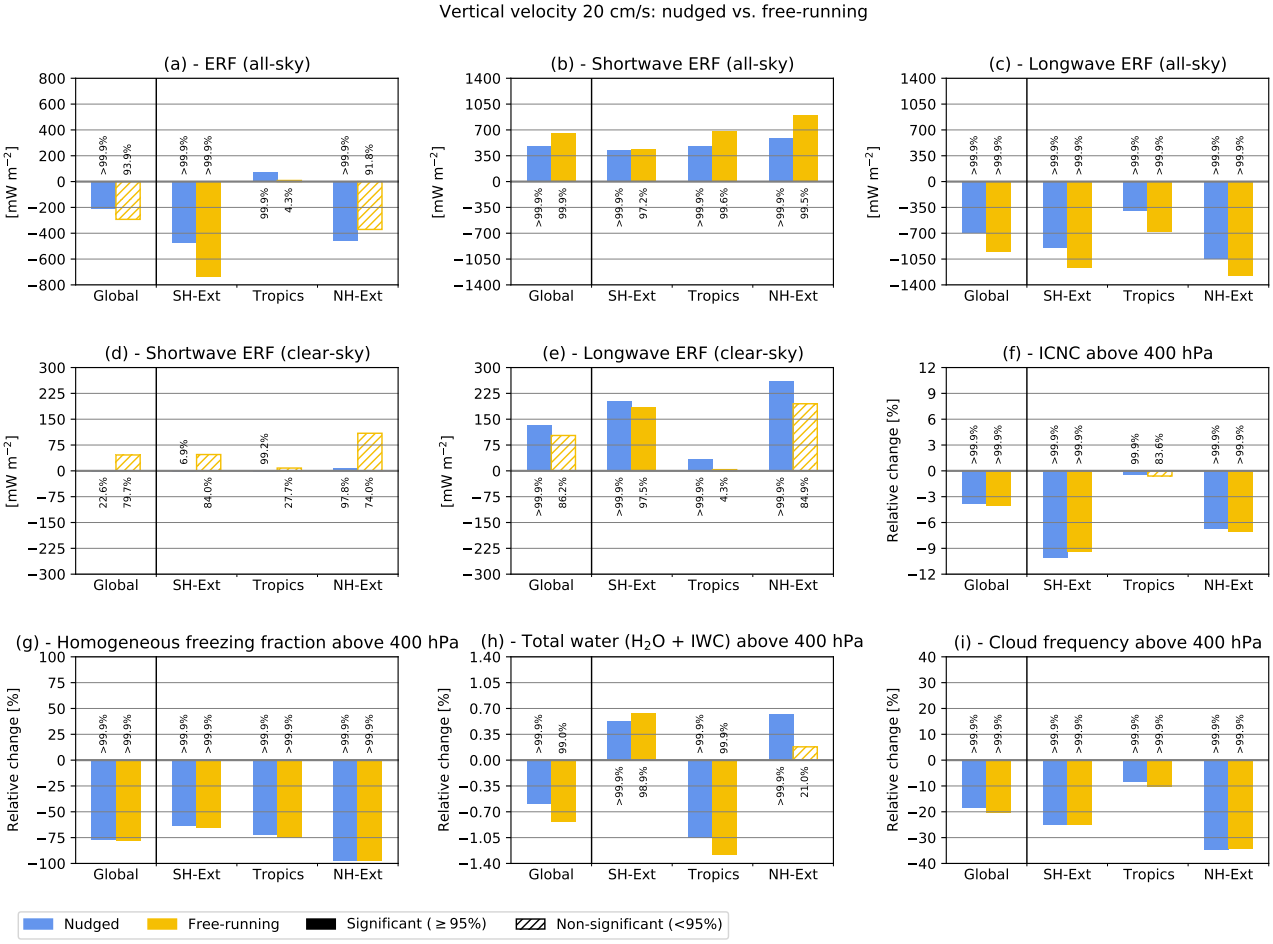

Figure S9. As in Fig. 1, but showing the total INP-cirrus effect for a prescribed vertical velocity of 20 $\mathrm{cm\,s^{-1}}$ simulated with a nudged (blue) and a free-running (yellow) model setup.

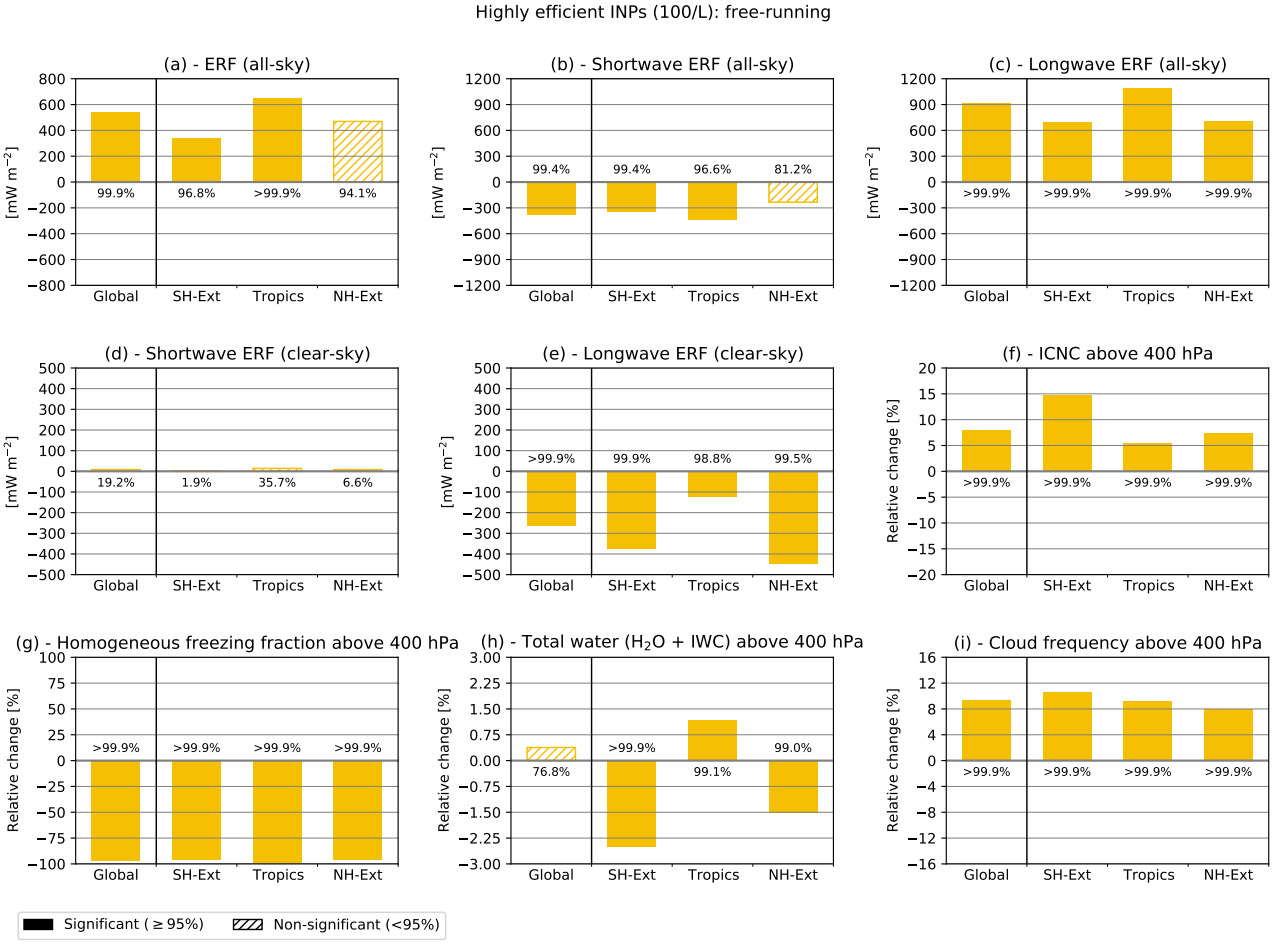

Figure S10. As in Fig. 1, but showing the INP-cirrus effect for highly efficient INPs ($100\,\mathrm{L}^{-1}$) for a free-running model setup.

References

Beer, C. G., Hendricks, J., Righi, M., Heinold, B., Tegen, I., Groß, S., Sauer, D., Walser, A., and Weinzierl, B.: Modelling mineral dust emissions and atmospheric dispersion with MADE3 in EMAC v2.54, Geosci. Model Dev., 13, 4287–4303, https://doi.org/10.5194/gmd-13-4287-2020, 2020.

Righi, M., Hendricks, J., and Beer, C. G.: Exploring the uncertainties in the aviation soot–cirrus effect, Atmos. Chem. Phys., 21, 17 267–17 289, https://doi.org/10.5194/acp-21-17267-2021, 2021.